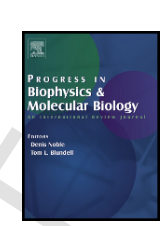


Contents lists available at ScienceDirect

### Progress in Biophysics and Molecular Biology

journal homepage: www.elsevier.com



# Multimodal on-axis platform for all-optical electrophysiology with near-infrared probes in human stem-cell-derived cardiomyocytes

Aleksandra Klimas <sup>a</sup>, Gloria Ortiz <sup>b</sup>, Steven Boggess <sup>b</sup>, Evan W. Miller <sup>b, c, d</sup>, Emilia Entcheva <sup>a,</sup>

- <sup>a</sup> Department of Biomedical Engineering, The George Washington University, Washington, DC, 20052, USA
- <sup>b</sup> Department of Chemistry, University of California, Berkeley, CA, 94720, USA
- <sup>c</sup> Department Molecular & Cell Biology, University of California, Berkeley, CA, 94720, USA
- <sup>d</sup> Helen Wills Neuroscience Institute, University of California, Berkeley, CA, 94720, USA

#### ARTICLE INFO

#### ABSTRACT

Article history:
Received 11 December 2018
Received in revised form 4 February 2019
Accepted 11 February 2019
Available online xxx

Combined optogenetic stimulation and optical imaging permit scalable, contact-free high-throughput probing of cellular electrophysiology and optimization of stem-cell derived excitable cells, such as neurons and muscle cells. We report a new "on-axis" configuration (combined single optical path for stimulation and for multiparameter imaging) of OptoDyCE, our all-optical platform for studying human induced pluripotent stem-cell-derived cardiomyocytes (hiPSC-CMs) and other cell types, optically driven by Channelrhodopsin2 (ChR2). This solid-state system integrates optogenetic stimulation with temporally-multiplexed simultaneous recording of membrane voltage ( $V_m$ ) and intracellular calcium ( $[Ca^{2^+}]_i$ ) dynamics using a single photodetector. We demonstrate the capacity for combining multiple spectrally-compatible actuators and sensors, including newer high-performance near-infrared (NIR) voltage probes BeRST1 and Di-4-ANBDQBS, to record complex spatiotemporal responses of hiPSC-CMs to drugs in a high-throughput manner.

© 2019.

#### 1. Introduction

Heart tissue is inherently dynamic, where a framework for both signal quantification and active interrogation is necessary to dissect the complex spatiotemporal phenomena underlying cardiac function (Entcheva and Bub, 2016). Contraction of the heart is driven by the propagation of electrical waves. At the cellular level, the triggering event, an action potential (AP), is determined by the balance of inward (depolarizing) and outward (repolarizing) ionic currents; the AP is closely followed by the increase in intracellular calcium concentration in the form of calcium transients (CTs), and ultimately calcium mediates mechanical contraction. To better understand electrical dysfunction, which can lead to complex electrical disturbances known as arrhythmias, optical mapping provides a means of contactless, high spatiotemporal recording of activity in cardiac tissue by employing fluorescent reporters. AP signals are obtained using fluorescent membrane voltage (V<sub>m</sub>) probes, such as the styryl dyes RH-237, Di-4-ANEPPS, and Di-8-ANEPPS, and intracellular calcium changes are captured by  $[Ca^{2+}]_{i}$  sensitive probes, such as Fura-2, Fluo-4 and Rhod-4, which typically provide stronger signals compared to the commonly used styryl-based V<sub>m</sub> probes (Entcheva and Bien, 2006; Herron et al., 2012). When combined with spectrally-compatible optogenetic actuators, such as the genetically encoded depolarizing ion channel Channelrhodopsin2 (ChR2) (Nagel et al., 2003) (Fig. 1a and

b), dynamic events in cardiac electrophysiology can be interrogated in a fully contactless, high-throughput dynamic manner (Klimas et al., 2016; Dempsey et al., 2016; McKeithan et al., 2017). Dynamic space-time patterns of light can be imposed for control of excitation waves in cardiac tissue (Burton et al., 2015). Optogenetic actuators can be combined with genetically-encoded sensors, such as the genetically-encoded calcium indicators (GECI) R-GECO (Zhao et al., 2011) (Fig. 1b) and the GCaMP-family of calcium sensors (Chen et al., 2013) (when a spectrally-compatible version of ChR2 is used). Furthermore, they can be combined also with voltage-sensitive fluorescent proteins (VSFP) such as VSFP3 (Mutoh and Knopfel, 2013), the QuasAr2 (Hochbaum et al., 2014), FlicR1 (Abdelfattah et al., 2016) and the ASAPs (Xu et al., 2018; Chamberland et al., 2017; St-Pierre et al., 2014; Lee and Bezanilla, 2017). Newer red-shifted near-infrared (NIR) voltage-sensitive dyes, producing superior optical signals, such as Di-4-ANBDQBS (Matiukas et al., 2007) and BeRST1 (Huang et al., 2015), not only expand the palette of available sensors combinable with optogenetic actuators, but also enable simultaneous recording of V<sub>m</sub> and [Ca<sup>2+</sup>]<sub>i</sub> of optically interrogated samples when using green-excited [Ca<sup>2+</sup>]<sub>i</sub> probes.

The traditional tools for probing cardiomyocyte electrophysiology with embedded parallelism, such as the planar patch clamp systems (Fertig and Farre, 2010) and microelectrode arrays (MEAs) (Li et al., 2016), rely on contact-based interrogation. Patch-clamp systems are often limited to isolated/single cells (Quach et al., 2018) and/or (non-cardiac) cell lines. MEAs can work with cardiomyocyte syncytia and can record tissue-level properties, such as conduction velocity, yet the need for contact and the extracellular voltage readout present limitations. In contrast, the contactless nature of all-optical platforms,

<sup>\*</sup> Corresponding author. Department of Biomedical Engineering, George Washington University, 800 22nd St NW, Suite 5000, Washington, DC, 20052, USA. Email address: entcheva@gwu.edu (E. Entcheva)

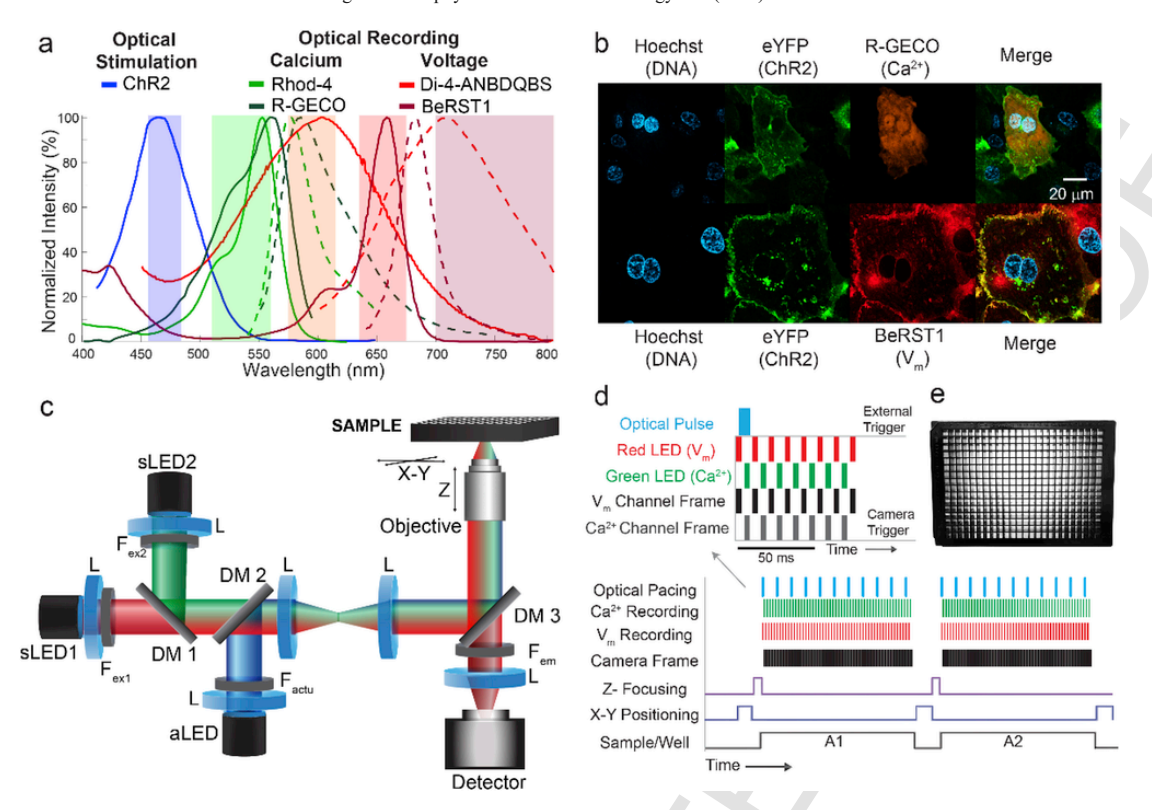


Fig. 1. "On axis" multimodal all-optical cardiac electrophysiology based on the OptoDyCE platform. (a) Spectrally-compatible synthetic and genetically-encoded fluorescent reporters of  $V_m$  and  $[Ca^{2^+}]_i$  can be combined with optogenetic actuators to perform all-optical interrogation of hiPSC-CMs. (b) Fluorescent images of hiPSC-CMs treated with the nuclear stain Hoechst (blue) show successful expression of both eYFP-tagged ChR2 (green) with R-GECO (orange), a genetically encoded  $[Ca^{2^+}]_i$  sensor, while the  $V_m$  dye BeRST1 (red) shows strong membrane localization. Scale bar is  $20\,\mu\text{m}$ . (c) OptoDyCE can readily perform simultaneous imaging of  $V_m$  and  $[Ca^{2^+}]_i$  using a single detector through 'strobing' the sensing LEDs (sLED1 and sLED2), which are temporally multiplexed or gated by the camera (d). Due to the contactless nature of all-optical interrogation, this approach allows for automated recording of standard multi-well plates (e). (For interpretation of the references to colour in this figure legend, the reader is referred to the Web version of this article.)

makes them suitable for probing of electrical activity in two- and three-dimensional constructs of human induced-pluripotent stem cells (hiPSC-CMs), i.e. allows them to investigate electrical activity within the tissue context. Our previously described system OptoDyCE exemplifies how optical mapping combined with optogenetics could be used to construct a low-cost, all-optical system for high-throughput cardiac electrophysiology. Here, we show the next generation of the OptoDyCE platform (Fig. 1c), where "on axis" design is used for optical stimulation and simultaneous  $V_m$  and  $[{\rm Ca}^{2^+}]_i$  imaging in hiPSC-CMs onto a single detector with "strobed" LED illumination, gated to specific camera frames (Fig. 1d). The "on axis" configuration refers to the combined single optical path leading up to the sample for stimulation and for the multiparameter imaging. The resultant system is compact and fully compatible with standard multi-well plates (Fig. 1e).

In order to characterize and demonstrate the flexibility of the system, we compare multiple  $V_m$  and  $[Ca^{2^+}]_i$  probes in hiPSC-CMs. In addition to the more commonly used NIR  $V_m$  sensor Di-4-ANBDQBS, we show the first full characterization of a new NIR probe, BeRST1, in optogenetically-paced hiPSC-CMs and demonstrate the compatibility of both sensors with ChR2 actuation as well as the  $[Ca^{2^+}]_i$  probes Rhod-4 and the genetically-encoded R-GECO. We assess the performance of the OptoDyCE platform and the utility of these probes for all-optical cardiac electrophysiology by quantifying spectral cross-talk due to the simultaneous use of multiple fluorescent probes and the stability of these probes under long-term, strobed illumination. To demonstrate the value of simultaneous dual imaging with high spatiotemporal resolution in the context of car-

diotoxicity testing, we explore cell-level uncoupling between  $V_m$  and  $[{\rm Ca}^{2^+}]_i$  in a known proarrhythmic compound, azimilide, in both spontaneous and optically-paced conditions. By fully characterizing the presented all-optical platform, we show that when combined with hiPSC-CMs or other scalable experimental cardiac models, OptoDyCE can provide a high-throughput means of standardization of protocols for electrophysiology testing across multiple sites (Yamamoto et al., 2016), cell sources (Blinova et al., 2017) as well as multiple testing platforms (Blinova et al., 2017; Harris et al., 2013) with a high number of replicates making high-throughput drug discovery, disease modeling, and personalized medicine realizable.

#### 2. Materials and methods

#### 2.1. Human iPS-cardiomyocyte culture and gene delivery

Culture of hiPSC-CMs and adenoviral delivery of ChR2(H134R) was performed as described previously (Klimas et al., 2016; Ambrosi et al., 2015; Ambrosi and Entcheva, 2014). Briefly, frozen human iPSC-derived cardiomyocytes (iCell Cardiomyocytes<sup>2</sup> TM, Cellular Dynamics International (CDI), Madison, WI) were thawed per the manufacturer's instructions and plated on fibronectin-coated wells in 384-well glass-bottom plates (Cellvis, Mountain View, CA), Fig. 1e, at the recommended plating density of 156,000 cells/cm<sup>2</sup> (17,000 cells/well for a 384 well plate). After 5 days, adenoviral delivery of ChR2(H134R)-eYFP to the iPSC-CMs was performed in-dish at a viral dose of MOI 350. Transfection of R-GECO (Addgene #45494 (CMV-R-GECO1.2) developed by Robert Campbell) was performed in-dish after delivery of ChR2. Briefly, Lipofectamine

3000 (ThermoFisher, Waltham, MA), P3000 (ThermoFisher), CDI iCell Plating Medium, and the R-GECO plasmid were combined per manufacturer's instructions and plasmid-containing solution remained in each well for at least 48 h. For all samples, functional testing was performed 2 days after transfection and/or infection.

## 2.2. All-optical recording of voltage and calcium under optogenetic pacing

Membrane voltage (V<sub>m</sub>) and intracellular calcium ([Ca<sup>2+</sup>]<sub>i</sub>) sensitive probes were administered, as described previously (Klimas et al., 2016; Chung et al., 2011; Jia et al., 2011). All experiments were performed at room temperature in Tyrode's solution containing the following (in mM): NaCl, 135; MgCl2, 1; KCl, 5.4; CaCl2, 1.33; NaH2PO4, 0.33; glucose, 5; and HEPES, 5 at pH 7.4. Optical recording of V<sub>m</sub> was performed using the new near-infrared synthetic dye BeRST1 (Huang et al., 2015) and Di-4-ANBDQBS (L. M. Loew) (Matiukas et al., 2007), while [Ca<sup>2+</sup>]<sub>i</sub> was reported optically with Rhod-4 or R-GECO. All probes were spectrally-compatible with ChR2. Dyes were diluted in Tyrode's solution to the desired optimized concentration as follows: BeRST1 (1 µM), Di-4-ANBDQBS (35 µM), and Rhod-4 (10 μM). Optical imaging was performed at >200 frames per second (fps) with  $4 \times 4$  binning with a field of view of  $\sim 0.4 \,\mathrm{mm}^2$ using NIS-Elements AR (Nikon Instruments: Melville, NY) on the OptoDyCE platform (Dempsey et al., 2016). Recordings of spontaneous and paced activity were obtained, where 5 ms, 0.5 Hz optical stimulation (470 nm) was provided using supra-threshold irradiances, as needed (in all cases < 1 mW/mm<sup>2</sup>).

A schematic of the system control and data acquisition protocol along with the light path of the optical system can be seen in Fig. 1, similar to that described previously (Klimas et al., 2016). The optical system (Fig. 1c) was built around an inverted microscope (Nikon Eclipse TE-2000) fitted with a programmable x-y stage and automated z-focus (Prior Scientific; Rockland, MA), with illumination for actuation and sensing using a custom-built adaptor. Illumination for sensing was provided by red (sLED1, 640 mW, at 660 nm) for voltage and green (sLED2, 350 mW, at 530 nm) for calcium, respectively, controlled by LED drivers (all parts from Thorlabs). Both LEDs were fitted with a bandpass filter: F<sub>ex1</sub>(Vm): FF655/ 40 nm (Semrock; Rochester, NY);  $F_{ex2}$  ([Ca<sup>2+</sup>]<sub>i</sub>): ET535/50 nm (Chroma; Bellows Falls, VT) and combined using a dichroic mirror DM1 (660 nm long-pass, Semrock). The actuation LED (aLED, 650 mW, 470 nm) for ChR2 was controlled using LED driver (Thorlabs) and fitted with a ET470/28 nm bandpass filter (Chroma), Factu. The light paths for optical sensing and actuation were combined by DM2 (495LPXR, Chroma) and directed to the sample using the appropriate dichroic DM3 for individual or simultaneous measurements (565DCXR, Chroma; 685-Di02, Semrock; 473/532/660rpc, Chroma). Irradiances between 0.3 and 6 mW/mm<sup>2</sup> for V<sub>m</sub> and 0.05–1 mW/mm<sup>2</sup> for [Ca<sup>2+</sup>]<sub>i</sub> were selected based on maximum signal strength while minimizing oversaturation of pixels and minimizing effects on ChR2 activation. Irradiances were chosen based on cell plating density and filter choice, but were kept constant over the course of a single experiment. In order to achieve simultaneous imaging, temporal multiplexing was used (Entcheva et al., 2004; Lee et al., 2011), where sLED1 and sLED2 were gated to each camera frame. Collimation optics comprised of several lenses (L), and an objective lens (in this case 20× Nikon CFI Super Plan Fluor, NA 0.75) was used to direct light to the sample. Emitted fluorescence was collected by a photodetector (iXon Ultra 897 EMCCD; Andor Technology Ltd., Belfast, UK) passing through the appropriate emission filter for individual or simultaneous measurements, F<sub>em</sub> (ET605/70m; 700LP; ET595/40m + 700LP, all Chroma). Illumination control was completely automated via software and TTL pulses. Illumination LEDs (sLED1 and sLED2) triggered off of the EMCCD camera (one LED on per frame during strobed illumination) and aLED was asynchronously controlled by an external TTL source (Fig. 1d).

#### 2.3. Drug preparation

Azimilide is a class III anti-arrhythmic drug used often in patients with implantable devices to slow down rhythm. Azimilide was diluted in DMSO (Sigma Aldrich) to achieve concentrations of  $0.01{-}10\,\mu\text{M}$  when diluted in Tyrode's solution. After the sample plates were loaded with dye(s), the Tyrode's wash solution was removed and replaced with Tyrode's solution containing the compound. The plates were then returned to the incubator  $(37\,^{\circ}\text{C},\,5\%\,\text{CO}_2)$  for 30 min prior to experiments to allow for equilibration.

#### 2.4. Data processing and analysis

Data was analyzed using software custom-developed in MATLAB (Entcheva and Bien, 2006; Klimas et al., 2016; Bien et al., 2006), and the following endpoints were extracted: peak, percent change in fluorescence ( $\Delta F/F\%$ ), and mean and standard deviation of baseline of  $V_m$  and  $[Ca^{2+}]_i$ . Signal-to-noise ratio (SNR) was calculated as ratio of peak signal to the standard deviation of the signal baseline. All data was averaged over the whole camera field of view ( $400\,\mu\text{m} \times 400\,\mu\text{m}$ ), unless otherwise specified. Pre-processing included baseline correction, removal of artifacts, temporal filtering using a Savitzky-Golay polynomial filter (second order, 3 frame window) and normalization (Bien et al., 2006).

#### 3. Results

#### 3.1. On-axis dual imaging system

The OptoDyCE system has been adapted to perform, for the first time, simultaneous dual imaging of voltage and calcium along with optogenetic stimulation using a single-detector, on-axis configuration (Fig. 1c). The choice of sensors and actuators is primarily limited by the spectral properties of the relevant chromophores (Fig. 1a). Currently, dye choice is dictated by the most popular blue-excited actuator ChR2. Many relevant sensors capable of excitation by LEDs have peak response when excited at wavelengths longer than that used for ChR2. These optical probes include the green-excited [Ca<sup>2+</sup>]<sub>i</sub> sensors Rhod-4 and the genetically-encoded R-GECO (Zhao et al., 2011) and near-infrared V<sub>m</sub> sensors, Di-4-ANBDQBS (Matiukas et al., 2007) and BeRST1 (Huang et al., 2015). The system was designed to work with these probes. The LEDs for exciting the sensors (sLED1, sLED2) and the actuator (aLED) along with bandpass filters used to narrow their spectra to prevent overlap  $(F_{ex1},\,F_{ex2},\,F_{actu})$  were selected based on the known absorption spectra. Likewise, this determined the selection of the dichroic mirrors (DM1, DM2, DM3) used to combine excitation sources and separate emitted photons before passing through the emission filters in front of the detector. Given the relatively low light levels required and the large selection of economically-priced light sources, a palette of probes can be used depending on spectral compatibility.

## 3.2. Compatibility of $V_m$ and $[Ca^{2+}]_i$ probes for dual imaging: crosstalk quantification

Simultaneous imaging using  $V_m$  and  $[Ca^{2+}]_i$  probes, including the genetically-encoded [Ca<sup>2+</sup>]<sub>i</sub> sensor R-GECO, reliably produces signals (Fig. 2a, c) with minimal crosstalk (Fig. 2b, d), demonstrating the applicability of the platform for multiparameter assessment of function. Crosstalk or "bleed-through" Di-4-ANBDQBS signal can be registered into the [Ca<sup>2+</sup>]<sub>i</sub> channel at this scale, likely due to minor motion artifacts (Fig. 2a, c). However the contribution (SNR and  $\Delta F/F(\%)$ ) of this artifactual signal is small compared to the Rhod-4 records. Although Di-4-ANBDQBS was reported to have an excitation spectrum spanning into that of the green LED (sLED2) (Fig. 1a), significant emission was not observed in this preparation. It should be noted that the provided spectra were obtained in ethanol, not in physiological solution (Hochbaum et al., 2014). Crosstalk of the remaining probes is negligible, with detector counts close to that of the dark counts of the EMCCD camera. Dual-strobing of dual-stained samples produced signals comparable in morphology to that of single-probe stained samples, both in terms of detector counts and  $\Delta F/F(\%)$ . Dual-strobing versus single strobing does produce some crosstalk, where the strong Rhod-4 is seen to bleed into on the  $\boldsymbol{V}_{m}$  channel (without green illumination) in single-stained samples (Fig. 2c and d), most likely the result of the non-zero decay time of the green LED and current source, which can be resolved by reducing the exposure time of the illumination LED. An interesting observation of increase in  $\Delta F/F(\%)$  and SNR for combined BeRST1 and Rhod-4 imaging (Fig. 2c and d) does not appear to be due to LED bleed-through, as the signal increase is observed under both single and dual strobing conditions and is specific to BeRST1 (not present for Di-4-ANBDQBS), and warrants further investigation. We argue that SNR provides a more informative metric for the quality of the optical signals compared to  $\Delta F/F(\%)$ , as seen when comparing V<sub>m</sub> and [Ca<sup>2+</sup>]<sub>i</sub> probes, where the voltage probes may produce lower  $\Delta F/F(\%)$  but the obtained signals have very high SNRs and require minimal post-processing.

## 3.3. Quantification of photobleaching and suitability of $V_m$ and $[Ca^{2+}]_i$ probes for long-term imaging

To determine the suitability of the synthetic  $V_m$  and  $[Ca^{2+}]_i$  probes for long term measurements, 5 min continuous recordings under strobed illumination were obtained in hiPSC-CM samples, optically paced at 0.5 Hz (Fig. 3). Bleaching occurs more strongly with Rhod-4 compared to the voltage probes (Fig. 3a and b), with a greater drop in  $\Delta F/F(\%)$  and SNR observed with Rhod-4 when comparing the first 20s and last 20s of the recording (Fig. 3b). BeRST1 exhibited excellent stability over time (hours), without any photobleaching within this 5-min record. Di-4-ANBDQBS had more baseline drift, most likely due to debris entering and exiting the field of view at this microscale; this was present to a lesser extent in BeRST1 samples, as this dye appeared to be less taken up by cellular debris. Even in the presence of bleaching, no major changes in signal morphology were observed with any of the three probes, and in all three cases SNR was high (Fig. 3c). None of the probes used in this study were found to result in any phototoxicity-induced changes in AP/CT morphology within the typical 1-3 h recording window.

#### 3.4. Spatiotemporal imaging

To demonstrate the utility of simultaneous dual imaging using OptoDyCE, hiPSC-CMs were treated with azimilide. The main target effect of this drug is anti-arrhythmic action (slowing rhythm in patients

with implantable devices). However, as azimilide blocks K+ ion channels, it can lead to undesired delays in repolarization, excessive prolongation of the action potential and its correlate - QT-interval in the electrocardiogram, and ultimately to repolarization-related arrhythmias; azimilide is considered a high-risk cardiotoxic compound (Gintant et al., 2016) for healthy patients or at elevated doses. Spontaneous and 0.5 Hz optical pacing recordings of hiPSC-CMs labeled with BeRST1 and Rhod-4 were obtained (Fig. 4). Although the azimilide-treated samples, Fig. 4b, showed AP and CT prolongation (known pro-arrhythmic markers) compared to DMSO control, Fig. 4a, no decoupling of voltage and calcium was observed in the global signal, averaged over the whole field of view. However, signals from sufficiently small ROIs at the single-cell scale show such decoupling of V<sub>m</sub> and [Ca<sup>2+</sup>]<sub>i</sub> (another pro-arrhythmic feature) in azimilide-treated samples, where abnormal activity in the spontaneous [Ca<sup>2+</sup>]<sub>i</sub> signal is not reflected in the V<sub>m</sub> signal. This highlights the need for simultaneous multiparameter measurements and for spatially-resolved imaging, which is particularly useful to distinguish between and gain mechanistic insights into calcium-triggered arrhythmic events vs. classic electrical instabilities (Shiferaw et al., 2005). Pacing can be effective in reducing this voltage-calcium decoupling and in suppressing abnormal calcium release events, yet the drug-induced AP prolongation limits the rates at which the system remains stable and responsive. Fig. 4c shows summary of results with azimilide treatment compared to control, namely significantly reduced frequency of spontaneous activations (p<0.01) and significantly prolonged action potential duration (APD) at 90% and at 50% recovery, p<0.01, for optically-paced records. Optical stimulation is essential for scalable measurements of drug-induced chages in the morphology of the action potentials and the calcium transients; even when a drug may act on the optogenetic actuator (ChR2), this has minimal effect on the measured APD, CTD, as we have suggested previously (Klimas et al., 2016). Optogenetic pacing is limited however, when probing changes in excitability if the tested drug has significant effects on ChR2.

#### 3.5. Effects of excitation irradiance on SNR

Although  $\Delta F/F\%$  is the most commonly reported quantification of signal quality in optical mapping, SNR plays a larger role in signal processing and feature detection. In this study with the presented platform, all probes showed excellent SNR. Even for very low light levels and low concentrations of staining, the optical signals were usable without filtering. The three probes characterized here were capable of SNR of 100 or more. Varying incident irradiance of the green LED for Rhod-4 excitation (Fig. 5a) shows that SNR only scales directly with irradiance until 0.3 mW/mm<sup>2</sup>, where oversaturation of pixels results in decreasing SNR. Multiple variables can affect the irradiances at which such saturation will be reached, including factors unrelated to the dyes used, e.g. camera pixel well depth and EM-CCD gain. It should be noted that the LED was set to only 30% maximum power (0.53 mW/mm<sup>2</sup>) before the whole detector area was oversaturated for these samples. Although ChR2 kinetics has been reported to be affected by green (520 nm) wavelengths (Bamann et al., 2008), mostly leading to accelerated closing of ChR2, peak SNR of Rhod-4 appears to occur at relatively low irradiances and thus excitation of the probe should not engage ChR2. Both Di-4-ANBDQBS and BeRST1 show similar profiles for irradiance (Fig. 5b and c). SNR for BeRST1 plateaus around 2.8 mW/mm<sup>2</sup>, while Di-4-ANBDQBS decreases in SNR at high LED irradiances >5.45 mW/mm<sup>2</sup> due to pixel oversaturation in areas with dye-containing cellular debris. For both V<sub>m</sub> probes, oversaturation of the whole detector area did not occur before the LED power was at maximum (6.6 mW/mm<sup>2</sup>). For most

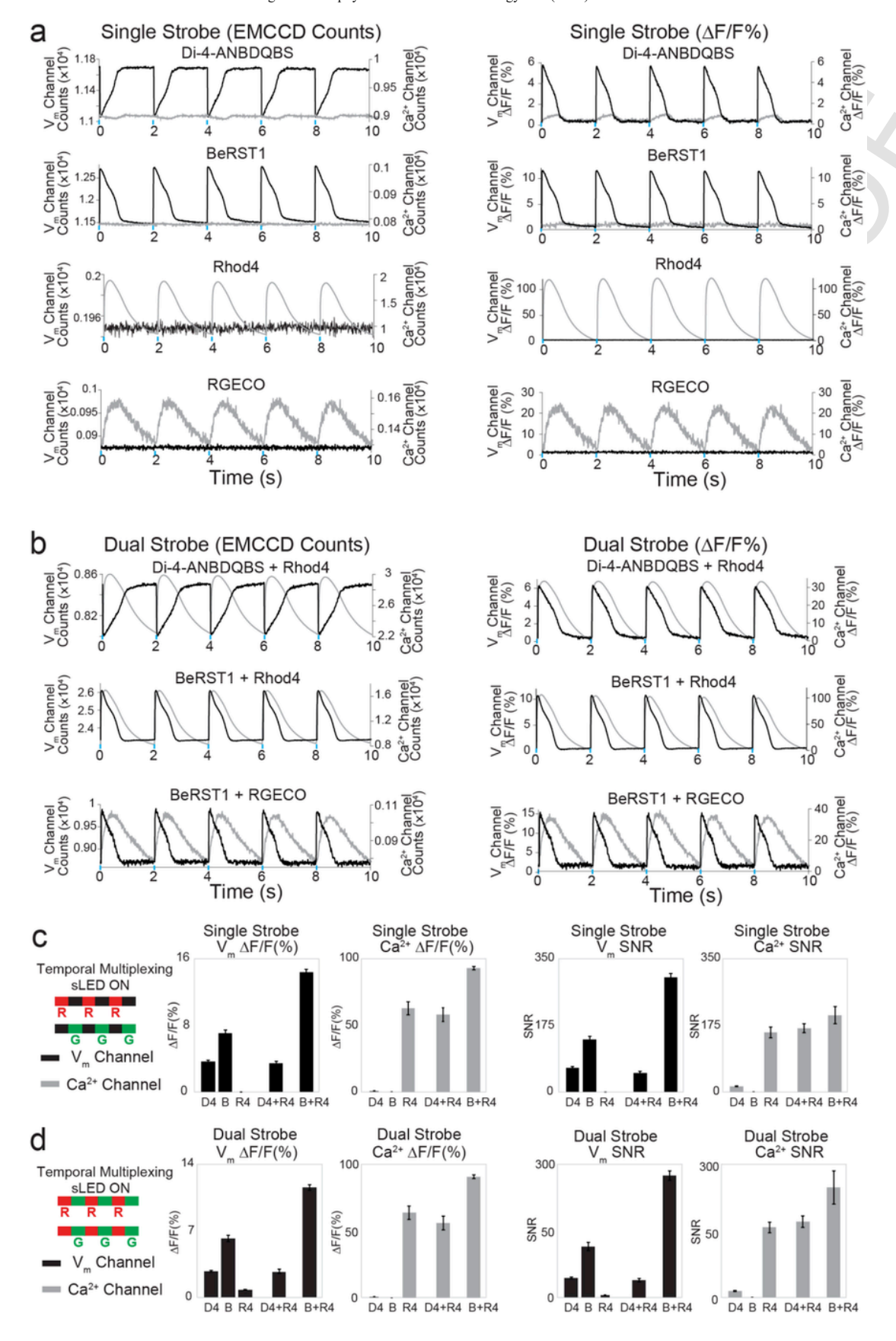


Fig. 2. Investigation of compatibility of  $V_m$  and  $[Ca^{2+}]_i$  probes and cross-talk. OptoDyCE can simultaneously measure  $V_m$  and  $[Ca^{2+}]_i$  using Di-4-ANBDQBS (D4) or BeRST1 (B) combined with Rhod-4 (R4) or RGECO (RG) under strobed illumination of hiPSC-CMs, optically paced at 0.5 Hz.  $V_m$  and  $[Ca^{2+}]_i$  channel denote recordings from frames gated to the excitation source (sLED) of the respective probes. Red (R) denotes recordings from frames synchronized to sLED1 ( $V_m$ ) and green (G) for sLED2 ( $[Ca^{2+}]_i$ ). Signals are given in terms of EMCCD detector counts (left) and  $\Delta F/F(\%)$  (right) for both single (a) and dual (b) strobe conditions. Single strobe illumination of single-probe samples (a, left) show counts close to the detector dark counts for B, R4, and RG while red-excited D4 is seen to produce a motion-artifact signal on the  $[Ca^{2+}]_i$  channel (green illumination). Comparison of  $\Delta F/F(\%)$  to SNR for both single-strobe and dual-strobe illumination (N=5, 6 distinct samples per case) (c,d) show that even if present, the SNR of the minor crosstalk is much smaller than that of the desired signal for the respective channel. Irradiances were kept the same for a particular wavelength (dye type) within a plate, but were adjusted between plates to account for differences in cell plating and dye loading and to optimize SNR; red LED: 1.4–2.5 mW/mm², green LED 0.46–0.53 mW/mm². (For interpretation of the references to colour in this figure legend, the reader is referred to the Web version of this article.)

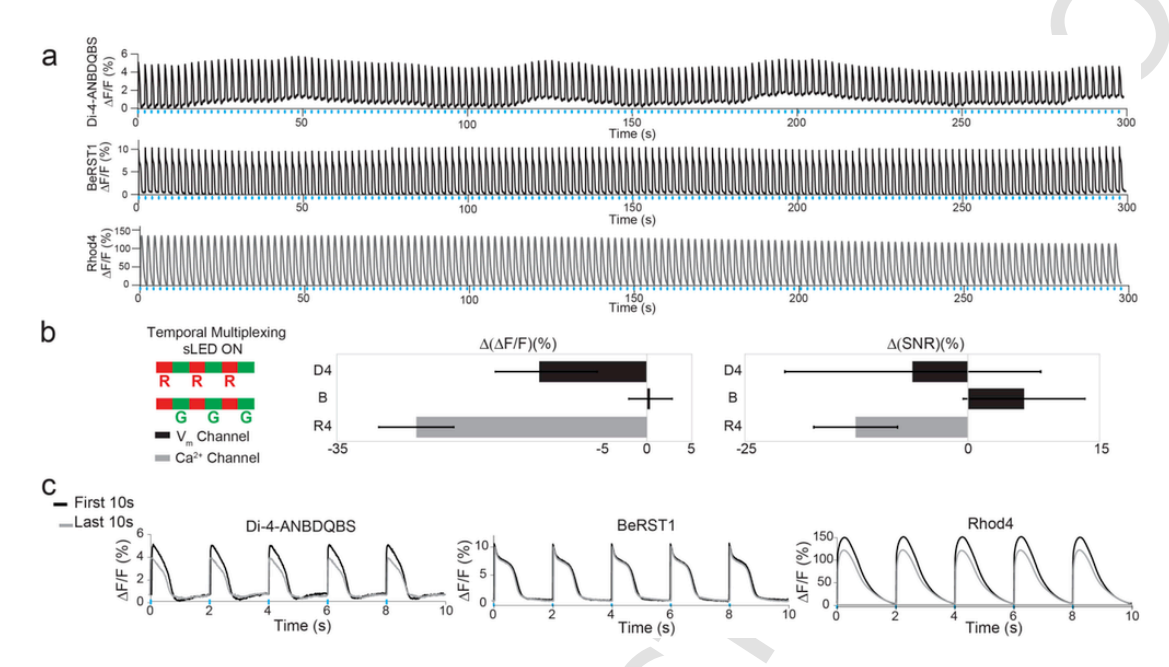


Fig. 3. Stability and photobleaching of  $V_m$  and  $[Ca^{2^+}]_i$  probes. Strobed illumination for 5 min combined with optical pacing exhibits minor photobleaching for di-4-ANBDQBS (D4) and Rhod4 (R4), but no photobleaching for BeRST1 (B) (a) with stronger bleaching observed in Rhod4 (R4) when comparing the percent change between the first and last 20 s of the recording for both  $\Delta F/F(\%)$  (given as  $\Delta$  ( $\Delta F/F$ )) and SNR (given as  $\Delta$  (SNR)) (N=4 samples) (b). Additionally, no major changes in AP/CT morphology are observed after 5 min of recording (c).

recordings, the relevant excitation irradiances for the calcium probes were lower than those for voltage probes, ranging from 0.46 to 0.53 mW/mm<sup>2</sup> for Rhod-4 and 1.4–2.5 mW/mm<sup>2</sup> for Di-4-ANBDQBS and BeRST1, as seen in (Fig. 5) and (Fig. 2c).

#### 4. Discussion

Here we demonstrate that OptoDyCE can be adapted to perform simultaneous dual imaging of V<sub>m</sub> and [Ca<sup>2+</sup>]<sub>i</sub> combined with optogenetic actuation using ChR2 to interrogate complex spatiotemporal phenomena in hiPSC-CMs. Although dual imaging approaches using a single detector and two LED sources have been proposed and employed previously, these systems relied on an "off-axis" configuration, where the illumination and detection paths do not overlap (Lee et al., 2011, 2012). While dual "on-axis" approaches have been performed, they typically rely on two-detector configurations (Fast and Ideker, 2000; Laurita and Singal, 2001; Choi and Salama, 2000). Considering that the photodetector (camera) is the most expensive component in these all-optical systems, the "on axis" temporal multiplexing approach presented here offers a particularly attractive solution. Additionally, none of the previously published techniques have demonstrated combined simultaneous measurements of V<sub>m</sub> and [Ca<sup>2+</sup>]<sub>i</sub> with optogenetic stimulation. Dual imaging using combined genetically-encoded sensors and actuators has been used to perform drug screening in hiPSC-CMs (Dempsey et al., 2016), however it required two cameras and two light sources for readout, and the actuators and sensors were not co-expressed in the same cells. Approaches using genetically-encoded probes and actuators are of interest in long-term monitoring of chronic drug treatment over hours and days, such as kinase-effecting drugs, where synthetic probes may not be ideal. OptoDyCE employs simple off-the-shelf optical components and uses temporal multiplexing of optical sensing by high-speed gating of LED illumination (Entcheva et al., 2004) not possible with traditional sources. Imaging of complex phenomena can be performed using a single detector thus achieving a cost-effective yet powerful configuration capable of acquiring high-content information. The "on-axis" aspect of the system makes it amenable to miniaturization and integration with micro-endoscopic systems for all-optical *in vivo* applications (Klimas and Entcheva, 2014).

As novel imaging technologies continue to be developed for use in cardiac electrophysiology, quality metrics for both the imaging system and the optical reporters must be established. Although optical mapping commonly uses  $\Delta F/F\%$  to determine the quality of a fluorescent reporter, we suggest that SNR provides a better metric of signal detectability and signal quality, which is more commonly used in the context of high-speed imaging. Given the need for recording speeds >200 fps (and thus short exposure times), signals with small (<10%) dynamic changes can be more susceptible to noise (e.g. detector and photon noise), requiring temporal and spatial filtering, which affects signal fidelity. When variability in the signal baseline is not taken into account, as with  $\Delta F/F\%$ , signal quality can be incorrectly represented, as seen when comparing  $V_m$  and  $[Ca^{2+}]_i$  probes

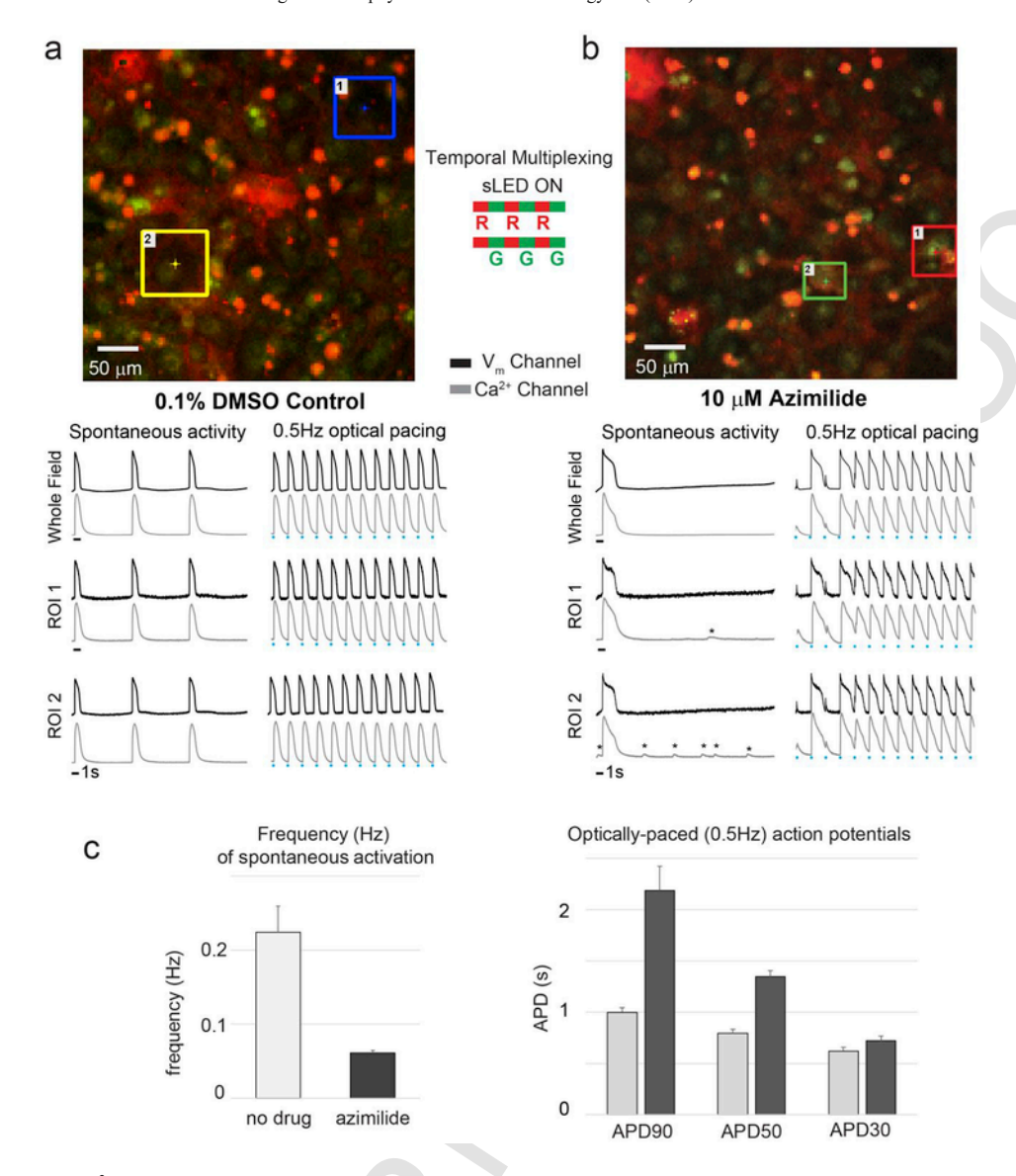


Fig. 4. Dual imaging of  $V_m$  and  $[Ca^{2^+}]_i$  probes to capture sub-cellular events for pro-arrhythmia prediction. hiPSC-CM samples stained with BeRST1 and Rhod-4 were treated with 0.1% DMSO (a) or  $10\,\mu\text{M}$  azimilide (b), a known proarrhythmic compound. Averaging over the whole field, azimilide is seen to prolong both the spontaneous and paced action potential and calcium transient, a known marker of pro-arrhythmic risk. Signals from single-cell ROIs show decoupling of  $V_m$  and  $[Ca^{2^+}]_i$  in azimilide treated samples (\*asterisks), another indicator of pro-arrhythmic risk, not detectable in the global signal. (c) Comparison of parameters for no-drug samples (N = 5) and azimilide (N = 6) - frequency of spontaneous activations (Hz) is decreased by azimilide; optically-paced (0.5 Hz) responses show prolonged action potential duration (APD) at 90, 50 and 30%.

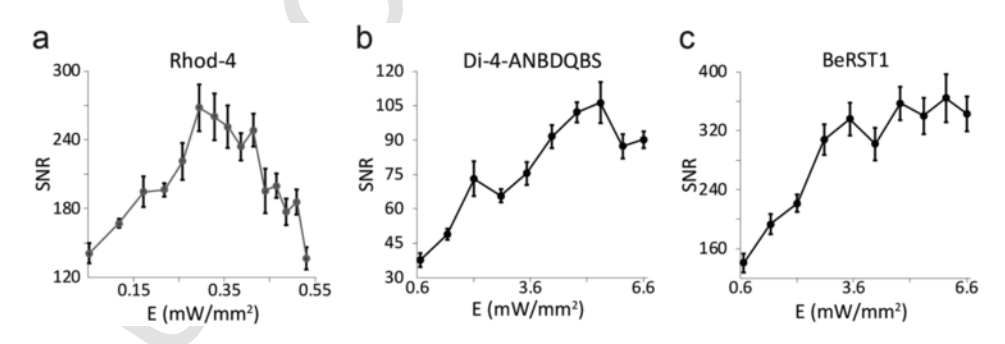


Fig. 5. Effects of excitation irradiance on SNR of  $V_m$  and  $[Ca^{2+}]_i$  probes. SNR for Rhod-4 (a), Di-4-ANBDQBS (b), and BeRST1 (c) were calculated for a single hiPSC-CM sample optically paced at 0.5 Hz.

(Fig. 2c and d). Additionally, we observe that  $\Delta F/F\%$  varies more than SNR across samples, most likely due to variability in dye loading and illumination intensity. Probes producing higher SNRs lessen the need for filtering signals, which both maintains signal fidelity and reduces computational requirements. It also reduces the strict dependence on expensive, high-sensitivity cameras and large numerical aperture (NA) optics. The recently synthesized near-infrared dye BeRST1 shows very high quality signals by both metrics and yields an impressive SNR, comparable to those for traditional [Ca<sup>2+</sup>]<sub>i</sub> probes. Di-4-ANBDQBS also provides a good readout. It is important to note that in their current formulations, BeRST1 required an order of magnitude lower concentration compared to Di-4-ANBDQBS (1 µM compared to 35 µM) to produce the signals presented here. However, further improvement of the SNR for Di-4-ANBDQBS and removal of the baseline drift may be possible by leveraging its capability as an excitation-ratiometric probe (Matiukas et al., 2007). When coupled with suitable photodetectors, sensitive in the NIR, these newer voltage sensors represent an important contribution to optical electrophysiology. They will fit a commercial need, as exemplified by recent developments and/or usage of NIR probes by several companies.

In all-optical electrophysiology, spectral compatibility and complex interactions between optical actuators and sensors present challenges when multiple variables need to be monitored simultaneously. Here, we demonstrate that simple solutions can be pursued, with minimal crosstalk, Fig. 2. Nevertheless, full characterization of potential interferences likely need to be conducted for each considered set of optical actuators and sensors, especially for genetically-encoded sensors, as ChR2 excitation is known to have the potential to photo-switch these sensors to different fluorescent states – a phenomenon that is enhanced at higher irradiance levels. For example, newer red-shifted GECI, jRCaMP1 and jRGECO1, were developed to minimize such effects (Dana et al., 2016).

The OptoDyCE platform is compatible with both synthetic and genetically-encoded sensors and allows for short-term and long-term all-optical control of samples with optogenetic actuators. In particular, the contactless nature makes the platform suitable for high-throughput measurements of hiPSC-CMs, allowing dissection of the V<sub>m</sub> [Ca<sup>2+</sup>]<sub>i</sub> dynamics. Although in this study we have only demonstrated OptoDyCE as a tool for measuring optically reported  $V_m$  and  $[Ca^{2+}]_i$  in hiPSC-CMs, the platform is suitable for recording any optically-measurable parameter (e.g. organelle-based ion concentrations, pH, contraction, etc.) and is impartial to the studied cell-type, allowing for the interrogation of compatible samples of different geometries, including 2D monolayers and small-thickness 3D tissue constructs for which light penetration is not limiting (Klimas et al., 2016). As new actuators and sensors (both synthetic and genetically-encoded) become available, they can be easily screened with and then integrated into the platform. The ability to provide dynamic pacing and high-throughput recording on an all-optical "on-axis" platform, easily adaptable to changing technologies, makes this an economical tool for better understanding of cardiac electrophysiology in vitro and in vivo. In the current in vitro context, it not only has the potential to improve cardiotoxicity testing, but also offers a cost-effective means of automation and phenotypic testing of hiPSC-CMs to accelerate the wider adoption of stem cell technologies in drug discovery and development, disease modeling, and personalized medicine.

#### Acknowledgements

This work was supported in part by the National Institutes of Health (grant numbers R01HL111649, R21 EB026152to E.E.; R35G-M119855 to E.W.M.) and the National Science Foundation (grants

1623068, 1705645, 1830941, 1827535to E.E.). E.W.M. acknowledges support from the Alfred P. Sloan Foundation (FG-2016-6359) and the March of Dimes (5-FY16-65). S.B. was supported in part by NIH T32GM066698. G.O. was supported in part by a Gilliam Fellowship for Advanced Study by the Howard Hughes Medical Institute.

#### References

- Abdelfattah, A.S., Farhi, S.L., Zhao, Y., Brinks, D., Zou, P., Ruangkittisakul, A., Platisa, J., Pieribone, V.A., Ballanyi, K., Cohen, A.E., et al., 2016. A bright and fast red fluorescent protein voltage indicator that reports neuronal activity in organotypic brain slices. J. Neurosci. 36, 2458–2472.
- Ambrosi, C.M., Entcheva, E., 2014. Optogenetic control of cardiomyocytes via viral delivery. Methods Mol. Biol. 1181, 215–228.
- Ambrosi, C.M., Boyle, P.M., Chen, K., Trayanova, N.A., Entcheva, E., 2015. Optogenetics-enabled assessment of viral gene and cell therapy for restoration of cardiac excitability. Sci. Rep. 5, 17350.
- Bamann, C., Kirsch, T., Nagel, G., Bamberg, E., 2008. Spectral characteristics of the photocycle of channelrhodopsin-2 and its implication for channel function. J. Mol. Biol. 375, 686–694.
- Bien, H., Yin, L., Entcheva, E., 2006. Calcium instabilities in Mammalian cardiomyocyte networks. Biophys. J. 90, 2628–2640.
- Blinova, K., Stohlman, J., Vicente, J., Chan, D., Johannesen, L., Hortigon-Vinagre, M.P., Zamora, V., Smith, G., Crumb, W.J., Pang, L., et al., 2017. Comprehensive translational assessment of human-induced pluripotent stem cell derived cardiomyocytes for evaluating drug-induced arrhythmias. Toxicol. Sci.: Off. J. Soc. Toxicol. 155, 234–247.
- Burton, R.A.B., Klimas, A., Ambrosi, C.M., Tomek, J., Corbett, A., Entcheva, E., Bub, G., 2015. Optical control of excitation waves in cardiac tissue. Nat. Photon. 9, 813–816.
- Chamberland, S., Yang, H.H., Pan, M.M., Evans, S.W., Guan, S., Chavarha, M., Yang, Y., Salesse, C., Wu, H., Wu, J.C., et al., 2017. Fast two-photon imaging of subcellular voltage dynamics in neuronal tissue with genetically encoded indicators.
  eLife 6.
- Chen, T.-W., Wardill, T.J., Sun, Y., Pulver, S.R., Renninger, S.L., Baohan, A., Schreiter, E.R., Kerr, R.A., Orger, M.B., Jayaraman, V., et al., 2013. Ultrasensitive fluorescent proteins for imaging neuronal activity. Nature 499, 295–300.
- Choi, B.R., Salama, G., 2000. Simultaneous maps of optical action potentials and calcium transients in Guinea-pig hearts: mechanisms underlying concordant alternans. J. Physiol. 529 Pt 1, 171–188.
- Chung, C.Y., Bien, H., Sobie, E.A., Dasari, V., McKinnon, D., Rosati, B., Entcheva, E., 2011. Hypertrophic phenotype in cardiac cell assemblies solely by structural cues and ensuing self-organization. FASEB J. 25, 851–862.
- Dana, H., Mohar, B., Sun, Y., Narayan, S., Gordus, A., Hasseman, J.P., Tsegaye, G., Holt, G.T., Hu, A., Walpita, D., et al., 2016. Sensitive red protein calcium indicators for imaging neural activity. eLife 5.
- Dempsey, G.T., Chaudhary, K.W., Atwater, N., Nguyen, C., Brown, B.S., McNeish, J.D., Cohen, A.E., Kralj, J.M., 2016. Cardiotoxicity screening with simultaneous optogenetic pacing, voltage imaging and calcium imaging. J. Pharmacol. Toxicol. Methods 81, 240–250.
- Entcheva, E., Bien, H., 2006. Macroscopic optical mapping of excitation in cardiac cell networks with ultra-high spatiotemporal resolution. Prog. Biophys. Mol. Biol. 92, 232–257.
- Entcheva, E., Bub, G., 2016. All-optical control of cardiac excitation: combined high-resolution optogenetic actuation and optical mapping. J. Physiol. 594, 2503–2510
- Entcheva, E., Kostov, Y., Tchernev, E., Tung, L., 2004. Fluorescence imaging of electrical activity in cardiac cells using an all-solid-state system. IEEE Trans. Biomed. Eng. 51, 333–341.
- Fast, V.G., Ideker, R.E., 2000. Simultaneous optical mapping of transmembrane potential and intracellular calcium in myocyte cultures. J. Cardiovasc. Electrophysiol. 11, 547–556.
- Fertig, N., Farre, C., 2010. Renaissance of ion channel research and drug discovery by patch clamp automation. Future Med. Chem. 2, 691–695.
- Gintant, G., Sager, P.T., Stockbridge, N., 2016. Evolution of strategies to improve preclinical cardiac safety testing. Nat. Rev. Drug Discov. 15, 457–471.
- Harris, K., Aylott, M., Cui, Y., Louttit, J.B., McMahon, N.C., Sridhar, A., 2013. Comparison of electrophysiological data from human-induced pluripotent stem cell-derived cardiomyocytes to functional preclinical safety assays. Toxicol. Sci.: Off. J. Soc. Toxicol. 134, 412–426.
- Herron, T.J., Lee, P., Jalife, J., 2012. Optical imaging of voltage and calcium in cardiac cells & tissues. Circ. Res. 110, 609–623.
- Hochbaum, D.R., Zhao, Y., Farhi, S.L., Klapoetke, N., Werley, C.A., Kapoor, V., Zou, P., Kralj, J.M., Maclaurin, D., Smedemark-Margulies, N., et al., 2014. All-optical electrophysiology in mammalian neurons using engineered microbial rhodopsins. Nat. Methods 11, 825–833.

- Huang, Y.-L., Walker, A.S., Miller, E.W., 2015. A photostable silicon rhodamine platform for optical voltage sensing. J. Am. Chem. Soc. 137, 10767–10776.
- Jia, Z., Valiunas, V., Lu, Z., Bien, H., Liu, H., Wang, H.Z., Rosati, B., Brink, P.R., Cohen, I.S., Entcheva, E., 2011. Stimulating cardiac muscle by LightClinical perspective cardiac optogenetics by cell delivery. Circulation: Arrhythmia and Electrophysiol. 4, 753–760.
- Klimas, A., Entcheva, E., 2014. Toward microendoscopy-inspired cardiac optogenetics in vivo: technical overview and perspective. J. Biomed. Optic. 19, 80701.
- Klimas, A., Ambrosi, C.M., Yu, J., Williams, J.C., Bien, H., Entcheva, E., 2016. OptoDyCE as an automated system for high-throughput all-optical dynamic cardiac electrophysiology. Nat. Commun. 7, 11542.
- Laurita, K.R., Singal, A., 2001. Mapping action potentials and calcium transients simultaneously from the intact heart. Am. J. Physiol. Heart Circ. Physiol. 280, 2053–2060.
- Lee, E.E.L., Bezanilla, F., 2017. Biophysical characterization of genetically encoded voltage sensor ASAP1: dynamic range improvement. Biophys. J. 113, 2178–2181.
- Lee, P., Bollensdorff, C., Quinn, T.A., Wuskell, J.P., Loew, L.M., Kohl, P., 2011. Single-sensor system for spatially resolved, continuous, and multiparametric optical mapping of cardiac tissue. Heart Rhythm 8, 1482–1491.
- Lee, P., Klos, M., Bollensdorff, C., Hou, L., Ewart, P., Kamp, T.J., Zhang, J., Bizy, A., Guerrero-Serna, G., Kohl, P., et al., 2012. Simultaneous voltage and calcium mapping of genetically purified human induced pluripotent stem cell-derived cardiac myocyte monolayers. Circ. Res.
- Li, X., Zhang, R., Zhao, B., Lossin, C., Cao, Z., 2016. Cardiotoxicity screening: a review of rapid-throughput in vitro approaches. Arch. Toxicol. 90, 1803–1816.
- Matiukas, A., Mitrea, B.G., Qin, M., Pertsov, A.M., Shvedko, A.G., Warren, M.D., Zaitsev, A.V., Wuskell, J.P., Wei, M.D., Watras, J., et al., 2007. Near-infrared voltage-sensitive fluorescent dyes optimized for optical mapping in blood-perfused myocardium. Heart Rhythm 4, 1441–1451.

- McKeithan, W.L., Savchenko, A., Yu, M.S., Cerignoli, F., Bruyneel, A.A.N., Price, J.H., Colas, A.R., Miller, E.W., Cashman, J.R., Mercola, M., 2017. An Automated platform for assessment of congenital and drug-induced arrhythmia with hipsc-derived cardiomyocytes. Front. Physiol. 8, 1–12.
- Mutoh, H., Knopfel, T., 2013. Probing neuronal activities with genetically encoded optical indicators: from a historical to a forward-looking perspective. Pflügers Archiv 465, 361–371.
- Nagel, G., Szellas, T., Huhn, W., Kateriya, S., Adeishvili, N., Berthold, P., Ollig, D., Hegemann, P., Bamberg, E., 2003. Channelrhodopsin-2, a directly light-gated cation-selective membrane channel. Proc. Natl. Acad. Sci. U. S. A. 100, 13940–13945.
- Quach, B., Krogh-Madsen, T., Entcheva, E., Christini, D.J., 2018. Light-activated dynamic clamp using iPSC-derived cardiomyocytes. Biophys. J. 115, 2206–2217.
- Shiferaw, Y., Sato, D., Karma, A., 2005. Coupled dynamics of voltage and calcium in paced cardiac cells. Phys. Rev. E - Stat. Nonlinear Soft Matter Phys. 71, 021903.
- St-Pierre, F., Marshall, J.D., Yang, Y., Gong, Y., Schnitzer, M.J., Lin, M.Z., 2014. High-fidelity optical reporting of neuronal electrical activity with an ultrafast fluorescent voltage sensor. Nat. Neurosci.
- Xu, F., Shi, D.Q., Lau, P.M., Lin, M.Z., Bi, G.Q., 2018. Excitation wavelength optimization improves photostability of ASAP-family GEVIs. Mol. Brain 11, 32.
- Yamamoto, W., Asakura, K., Ando, H., Taniguchi, T., Ojima, A., Uda, T., Osada, T., Hayashi, S., Kasai, C., Miyamoto, N., et al., 2016. Electrophysiological characteristics of human iPSC-derived cardiomyocytes for the assessment of drug-induced proarrhythmic potential. PLoS One 11, e0167348.
- Zhao, Y., Araki, S., Wu, J., Teramoto, T., Chang, Y.F., Nakano, M., Abdelfattah, A.S., Fujiwara, M., Ishihara, T., Nagai, T., et al., 2011. An expanded palette of genetically encoded Ca2+ indicators. Science 333, 1888–1891.